Professional Research Assistants

Category: Graduate Students
Poster # PRA1

Title: Evaluation of Azobenzene Nanogels in Adhesive Dentistry

Dixa Gautam, Gannon Kehe, Humberto Escobedo, Devatha Nair

Purpose: The aim of this study was to synthesize, characterize, and evaluate an azobenzene nanogel and its ability to reduce bacterial invasion of cariogenic biofilms while preserving the mechanical strength and structural integrity within adhesive resins.

Methods: To synthesize the azobenzene nanogel, 4-hydroxyazobenzene and hexamethylene diisocyanate were homogeneously mixed in a round bottom flask with 4x-toluene using dibutyltin dilaurate as the initiator. Glycerol and 2-isocyanatoethyl methacrylate were added at the 10-minute mark and the solution polymerization was allowed to proceed at room temperature for 12 hours until 100% conversion was observed. Contact angle, water sorption/solubility, degree of conversion, viscosity, and microtensile bond strength of the nanogel dispersed in a 40:60:12 *BisGMA: HEMA: Ethanol* formulation were tested at 3 different concentrations (0.5, 1.5, and 2.5 wt.%). Substrates were polymerized with an LED curing light for 2 minutes on each side at 700mW/cm^2 using Camphorquinone (CQ) and ethyl 4-N,N-dimethylaminobenzoate (EDMAB) as photoinitiators. A second dual-cure initiating system consisting of benzoyl peroxide and dimethyl-p-toluidine (in addition to CQ+EDMAB) was also tested, allowing polymerization to be limited to a total of 40 seconds, reflecting a more clinically relevant timescale. Subsequently, two antibacterial tests were run including an MTT assay as a means to test extractable and leachable and a direct test where S. mutans were seeded on the adhesive substrates.

Results: Azobenzene nanogel networks showed improved hydrophobicity with a ≥ 25˚ increase in water contact angle ($P < 0.0001$) at low concentrations of the azobenzene nanogel. The polymerized adhesive surfaces formulated with azobenzene nanogels showed a 66% reduction ($P < 0.0001$) in bacterial biofilms relative to the control while maintaining the mechanical properties and micro-tensile bond strength of the adhesive networks.

Sample type	Degree of Conversion Method 1 (%) (n=3)	Degree of Conversion Method 2 (%) (n=3)	Contact Angle (°) (n=3)	Solubility (µg/mm^3) (n =3)	Sorption (µg/mm^3) (n =3)	CFUs on Substrate (*10^8) (n = 15+)
Control	97.3 ± 1.06	98.6 ± 0.3	28 ± 1	-78 ± 15	8 ± 3	11.1 ± 4.4
0.5 wt.%	96.7 ± 0.81	98.6 ± 0.3	56 ± 6	-82 ± 13	10 ± 1	5.79 ± 1.9
1.5 wt.%	97.9 ± 1.04	98.0 ± 0.2	58 ± 2	-65 ± 5	9 ± 4	3.74 ± 1.5
2.5 wt.%	97.6 ± 0.6	98.2 ± 0.5	53 ± 2	-59 ± 7	7± 2	3.88 ± 1.9

Conclusions: The increased hydrophobicity and antibacterial activity are promising indicators that azobenzene nanogel additives have the potential to increase the durability and longevity of adhesive resins.

Category: Graduate Students
Poster # PRA2

Title: Conditioned Media from PKCδ Depleted Cells is Sufficient to Transfer Radioprotection

Ami Haas, Ella Annest, Angela Ohm, Trisiani Affandi, Aaron V. Issaian, and Mary E. Reyland

Purpose: Despite improvements in irradiation (IR) delivery, up to 40% of patients treated with (IR) for head and neck carcinoma (HNC) will develop moderate to severe xerostomia as a result of damage to the salivary glands in the IR path. Salivary gland hypofunction, and the resultant xerostomia, is permanent and can have a significant impact on oral health and nutrition. Our lab has previously shown that protein kinase C delta (PKCδ) is essential for IR-induced apoptosis, and that inhibition or loss of PKCδ protects salivary gland function in a mouse model of head and neck IR. Irradiated cells have been shown to secrete factors to regulate the survival of unirradiated cells in the vicinity (radiation-induced bystander effects). *We have investigated the hypothesis that protection provided by inhibition of PKCδ can be transferred to surrounding cells by a similar mechanism.*

Methods: For these studies, we used rat salivary acinar cells (Par-C5) depleted of PKCδ by expression of shRNA to PKCδ and Par-C5 cells expressing a non-targeting shRNA. Conditioned media (CM) was collected after 24 hrs. and transferred to naïve Par-C5 cells.

Results: We show that radioprotection can be transferred to naïve Par-C5 cells through CM collected from PKCδ depleted cells (shPKCδ CM). shPKCδ CM increases proliferation and colony formation while decreasing apoptosis in response to IR. Mechanistically, this results from increased DNA repair and is associated with alterations in mitochondrial oxidative phosphorylation. Proteomic analysis of shPKCδ CM reveals increased antioxidants and metabolic enzymes associated with the pentose phosphate pathway. This pathway is important for antioxidant production and the synthesis of nucleotides for DNA repair.

Conclusions: CM provides radioprotection to naïve Par-C5 cells through a mechanism that involves increased DNA repair. Identification of the active factor in shPKCδ CM might suggest new therapeutic approaches for radioprotection.

Funding Source: NIH/NIDCR R01DE015648 and R01DE027517 to MER

Category: Professional Research Assistant
Poster # PRA3

Title: Glassy Elastomeric Photopolymers for Enhanced Strength, Toughness and Resilience

Gannon Kehe, Austyn Salazar, Matthew Barros, Jeffrey Stansbury

Purpose: Investigate the urethane-acid functional group interaction in polymers by employing low molecular weight polycaprolactone (PCL) core structures functionalized as urethane methacrylates. Photocurable resins were formulated by supplementing the PCL-based monomers with methacrylic acid to study polymeric mechanical properties based on the systematic variation of the urethane to acid functional group proportionality.

Methods: A polycaprolactone diol and triol were reacted with functional group molar equivalents of 2-isocyanatoethyl methacrylate to form urethane methacrylate monomers. The reactive PCLs were then formulated with methacrylic acid (MAA) at 1:1, 1:1.5, 1:2 and 1:3 urethane to acid functional group ratios, photopolymerized with a 365nm light at 100 mW/cm^2, and post cured to high conversion with elevated temperature (80

°C°C

) and light (365nm/405nm) for 1 hour (n = 7) (Dimensions 25x2x2). The mechanical properties of these polymers were then assessed via three-point bend testing taken either to failure or halted at the deflection limit. Selected specimens were submitted to multiple loading/unloading cycles to progressively higher strain.

Results:

Table 1: Mechanical Properties of Polymers

Resin formulation	Modulus (GPa)	Flexural Strength (MPa)	Toughness (MPa)
PCL diurethane dimethacrylate homopolymer	0.04 ± 0.003	4.7 ± 0.6	0.7 ± 0.2
PCL diurethane dimethacrylate : MAA 1:1	0.53 ± 0.04	27.4 ± 0.8	5.2 ± 0.8
PCL diurethane dimethacrylate : MAA 1:1.5	1.43 ± 0.12	71.6 ± 4.2	12.2 ± 1.2
PCL diurethane dimethacrylate : MAA 1:2	1.81 ± 0.08	88.6 ± 3.0	12.8 ± 1.0
PCL diurethane dimethacrylate : MAA 1:3	2.63 ± 0.08	130.5 ± 4.2	21.1 ± 1.1
PCL triurethane trimethacrylate : MAA 1:1	3.57 ± 0.19	166.9 ± 24.3	12.0 ± 7.1

All moduli were statistically significant compared to each other (One-Way ANOVA $P<0.0001$). All Flexural Strengths were statistically significant compared to each other $P<0.05$)

Conclusion: By variation of the urethane to acid ratio, which also alters the covalent network density, substantially enhanced modulus, flexural strength, and toughness of these PCL-based urethane materials was demonstrated. These polymers also

displayed an unusual combination of stiffness and flexibility with resilient tolerance to extensive deformation. Some of these photopolymers appear appropriate for dental applications of 3D printing.
Funding Source: NIH/NIDCR R21DE028444

Category: Professional Research Assistant
Poster # PRA4

Title: Eradication of *Streptococci* and Oral Biofilm Removal through Photoresponsive Acrylated HydroxyAzobenzene (AHA) Coatings

Gannon Kehe, Sarah Asby, Audelia Castro, Michael Schurr, Chaitanya Puranik, Devatha Nair

Purpose: Develop dynamic, photoresponsive, Acrylated HydroxyAzobenzene (AHA) surface coatings, for dental restorations, that selectively kills streptococcus in a multi-species biofilm, which may then photomechanically disrupt and remove oral biofilms via the photofluidization of the azobenzene moieties.

Methods: Kill curves for *Streptococcus mutans* (SM) and *Streptococcus oralis* (SO) were generated by diluting liquid cultures (n=3) of each species to 10^5 CFUs/mL and 1 mL was seeded on AHA substrates and uncoated controls (n = 3). The media was sampled every hour and live bacterial concentration in CFUs/mL was quantified via serial dilutions with 3 technical replicates seeded on BHI agar plates. Salivary bacteria was collected from two separate subjects, combined and concentrated, and light treatment oral microbiome biofilm removal studies were conducted by seeding 10^6 CFUs/mL on AHA coated and uncoated resin substrates. Biofilm formation was allowed to occur for 8 hours and the substrates were subsequently irradiated with a 3M™ Elipar™ LED Curing Light to induce photofluidization of the surface coating and mechanical disruption of the biofilm. The substrates were then gently washed in sterile 1X PBS. This process was repeated twice and the substrates were then sonicated to determine the amount of biofilm remaining. The PBS from washes and sonication were quantified via serial dilutions and initial and final CFUs was assessed.

Results:

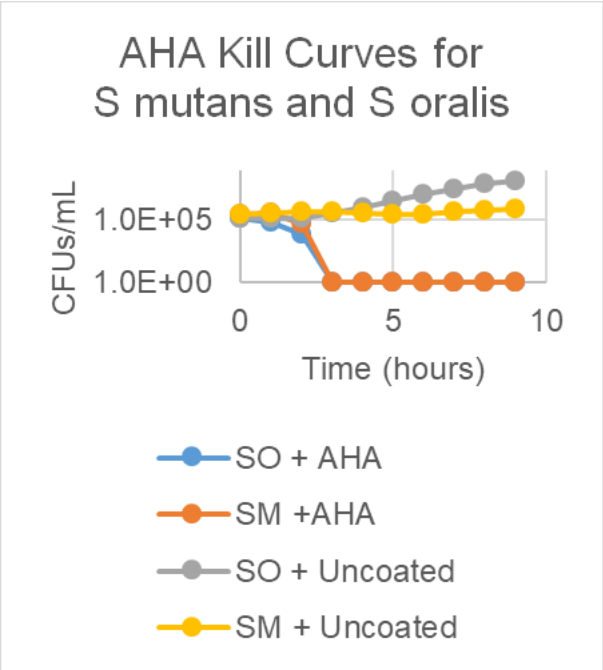

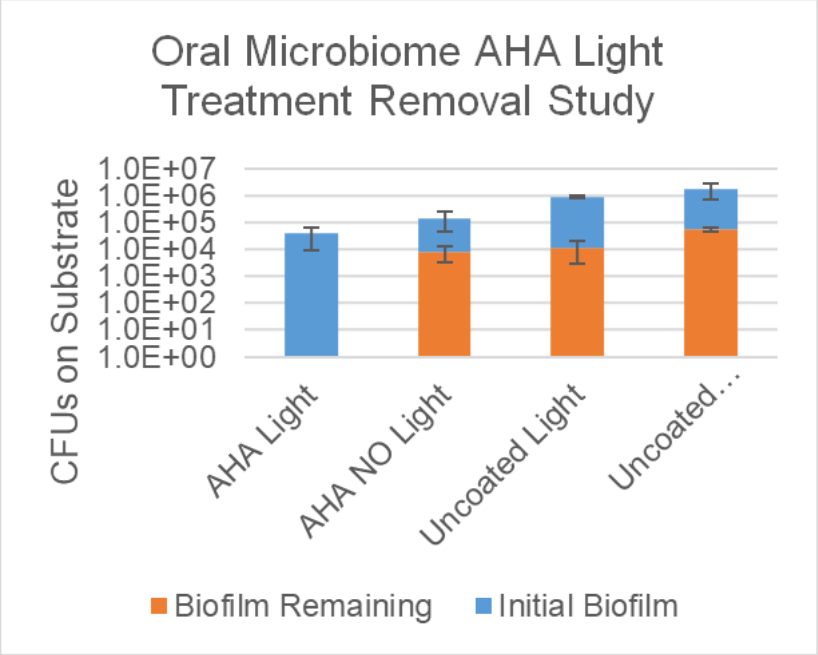

Statistical significance for Kill Curves between AHA substrates and Uncoated controls was achieved at t=2 hours for SM and t=7 hours for SO. 2-Way ANOVA (AHA v Uncoated $P<0.0001$).

Conclusions: By selectively eliminating streptococcus from the oral microbiome consortium, we demonstrate the ability to effectively remove 100% of the biofilm formed on the AHA- coated substrates. This was achieved via a photomechanical disruption of the oral biofilms through the photofluidization of AHA by irradiation with a common dental lamp.

Funding Source: NIH-NIDCR K25DE027418 and NIH –NHLBI U01HL152405

Category: Graduate Students
Poster # PRA 5

Title: *mef2cb* Buffers Against *mef2ca* Loss in the Zebrafish Craniofacial Skeleton

Matthew Murry, Raisa Bailon-Zambrano, Juliana Sucharov-Costa, James T. Nichols

Purpose: A significant portion of craniofacial structures are derived from the neural crest, a transient population of cells of ectodermal origin that undergo a mesenchymal transformation to migrate ventrally and form a multitude of structures, including the cartilaginous precursors to facial bone. The MEF2C gene family is understood to be functionally required for normal neural crest development in both human and zebrafish. Humans with MEF2C haploinsufficiency syndrome present variable facial dysmorphologies. Although zebrafish *mef2ca* mutants have well-characterized craniofacial defects, the functional contribution of its closest-related paralog, *mef2cb,* is much less understood.

Methods: Zebrafish *mef2cb* mutants were evaluated both individually and in combination with *mef2ca* for the severity and variation of various craniofacial phenotypes. Fischer's exact test was used to evaluate phenotypic significance between craniofacial cartilage and bone of different genotypes. Studies with symplectic cartilage measurements are presented as box and whisker plots, the box extends from the 25th to 75th percentiles. The line in the middle of the box is plotted at the median and the bars are minimum and maximum values. A Dunnet's T3 test was used to compare total symplectic cartilage (left plus right sides) between genotypes.

Results: *mef2cb* single mutant fish produced no overt phenotype, however, loss of one copy of *mef2cb* in *mef2ca* homozygous mutants and loss of both copies of *mef2cb* in *mef2ca* heterozygotes enhanced the severity and variability of the *mef2ca* craniofacial phenotype.

C

mef2cb-/- low-penetrance strain	*mef2ca +/+* n=30 mutants	*mef2ca +/-* n=21 mutants
mef2ca- phenotype	penetrance	
ectopic op bone:	0%	0%
ih joint fusion:	0%	14%
dysmorphic ch:	0%	14%
reduced mc:	0%	14%
jaw joint fusion:	0%	14%
shortened sy:	0%	29% *

–

mef2ca-/- low-penetrance strain	*mef2cb +/+* n=12 mutants	*mef2cb +/-* n=21 mutants
mef2ca- phenotype	penetrance	
ectopic op bone:	17%	79% *
ih joint fusion:	92%	100%
dysmorphic ch:	58%	96% *
reduced mc:	67%	96% *
jaw joint fusion:	83%	100%
shortened sy:	100%	100%

Figure 1. Phenotype scoring of *mef2ca;mef2cb* genotype combinations.

Conclusions: These findings demonstrate that *mef2cb* can buffer against loss of *mef2ca* severity in the context of deleterious mutations and broadens the understanding of how the MEF2C family acts to regulate craniofacial development.

Funding Sources: NIH R01 DE029193

Category: Professional Research Assistant
Poster # PRA6

Title: PKCδ Regulates Mitochondrial Energy Production

Angela Ohm, Jordan Speidel, Dillon Boulton, Cecilia Caino, Angelo D'Alessandro, and Mary E Reyland.

Purpose: Our lab has previously shown that protein kinase C delta (PKCδ) is essential for IR-induced apoptosis, and that inhibition of PKCδ protects salivary gland function through a mechanism that involves regulation of DNA repair. Mitochondria dysfunction and alterations in metabolism can contribute to DNA damage repair by multiple mechanisms, including regulation of ATP production, nucleotide synthesis and chromatin remodeling. *Here we have investigated the hypothesis that loss of PKCδ alters cellular metabolism and mitochondrial function.*

Methods: We compared metabolism, and mitochondrial function and structure in rat salivary acinar cells (Par-C5) depleted of PKCδ by expression of shRNA (shPKCδ) to Par-C5 cells expressing a non-targeting shRNA (shNT).

Results: Our studies show that metabolic pathways that regulate nucleotide, amino acid and antioxidant synthesis are most highly affected by depletion of PKCδ. This suggests that depletion of PKCδ may reprogram cells to increase DNA repair and reduce oxidative DNA damage. To explore the mechanistic basis for these changes, we examined mitochondrial energy production. Loss of PKCδ decreased oxygen consumption and ATP production, and increased ROS, suggesting a defect in the mitochondrial electron transport chain (ETC). Further analysis showed that expression of key proteins in ETC complexes 1, 2 and 4 are reduced, and that complex 1 function is reduced. Mitochondrial fission facilities the removal of damaged mitochondria and can be detected by structural changes in mitochondria such as fragmentation. We show that loss of PKCδ results in an increase in fragmentation of mitochondria which is accompanied by increased expression and phosphorylation of the fission regulator, Drp1.

Conclusion: Together our studies support a role for PKCδ in regulation of mitochondria homeostasis and provide insight into how inhibition of PKCδ may rewire cells to maximize survival under conditions of cell damage.

Funding Source: NIH/NIDCR R01DE015648 and R01DE027517 to MER

Category: Professional Research Assistant
Poster # PRA7

Title: High Performing Tetraurethane (Meth)acrylate Photopolymer Formulations

Austyn Salazar, Matt Barros, Gannon Kehe, Jeff Stansbury

Purpose: This study investigates novel urethane (meth)acrylates as comonomers with (meth)acrylic acid to further understand the potential reinforcing effects of non-covalent interactions on polymeric mechanical properties.
Methods: Tetraurethane di(meth)acrylate TUD(M)A comonomers were synthesized and combined with (meth)acrylic acid (M)AA at a 1:1 or 2:1 ratio of the acid to urethane functional groups. The formulations were photocured (365nm; 100mW/cm^2) and post cured using a combination of light (365nm/405nm) and heat (80°C) with conversion measured by FT-IR and polymeric flexural strength, modulus and toughness were obtained in 3-point bending using n=7 samples.
Results: The TUD(M)A/(M)AA polymers displayed extremely high flexural strength and modulus. To highlight the synergistic reinforcing effect of the acid-urethane hydrogen bonding, the TUDMA homopolymer has a flexural strength of 86.5±4.3 MPa and a modulus of 2.1±0.2 GPa. The resin viscosities are relatively high (>100 mPa*s); however, increasing the acidic comonomer content enables a substantial drop in viscosity while maintaining mechanical properties. These good properties are available in both methacrylate and acrylate compositions with the latter providing higher reactivity and conversion. A formulation consisting of TUDMA with an extended spacer between the urethane and methacrylate group (TUDMA$_{ext}$) provided the highest flexural strength while the acrylate-containing polymers produced the best toughness values.

Table 1: Mechanical Characterization of Polymers

	Acid:Urethane Molar Ratio	Flexural Strength (MPa)	Modulus (GPa)	Toughness (MPa)	Viscosity (mPa*s)	Conversion (%)	
						UV	Post cure
TUDMA + MAA	1:1	235 ± 20.0	5.26 ± 0.36	7.2 ± 1.5	552 ± 108	61.7 ± 0.2	85.9 ± 0.1
TUDMA + MAA	2:1	212.5 ± 20.0	5.18 ± 0.17	5.9 ± 1.4	39.2 ± 3.9	63.4 ± 2.7	83.1 ± 1.0
TUDMA + AA	1:1	250.2 ± 8.6	5.18 ± 0.17	19.1 ± 7.5	254.3 ± 26.1	83.1 ± 2.0	95.6 ± 0.1
TUDA + AA	1:1	206.0± 12.2	5.14 ± 0.32	23.0 ± 9. 4	145.4 ± 17.2	90.2 ± 1.2	96.4 ± 0.7
TUDA + AA	2:1	207.6 ± 18.3	5.28 ± 0.42	23.7 ± 13.8	37.1 ± 4.87	96.5 ± 0.6	98.4 ± 0.01
$TUDMA_{ext}$ + MAA	1:1	258.6 ± 12.0	4.94 ± 0.12	12.0 ± 2.2	246.8 ± 54.3	73.3 ± 0.5	91.7 ± 0.5
UDMA	N/A	157.6 ± 6.5	3.13 ± 0.12	2.2 ± 1.4	8912 ± 104	*	*
UDMA + MAA	1:1	179.7 ± 25.0	4.14 ± 0.31	2.9 ± 1.1	118 ± 3.0	*	*

Conclusions: These novel copolymers display high flexural strength (>200 MPa), high modulus (5 GPa), and moderate to high toughness. This study shows the potential for high performing materials via non-covalent bonding reinforcement of photopolymer networks.

Funding Source: NIH/NIDCR R21DE028444

Category: Professional Research Assistant
Poster # PRA8

Title: ***her9* is required for neural crest cell derived dermal bone development**

Amanda Stenzel, Juliana Sucharov, Bruce Appel, James T. Nichols

Purpose: The Jagged-Notch signaling pathway has been shown to play a role in craniofacial patterning. Well known targets of the Jagged-Notch signaling pathway include the Her/Hes family. In humans, mutations in HES4 is associated with chromosome 1p36 deletion syndrome. Characteristics of chromosome 1p36 deletion syndrome are microbrachycephaly and midface hypoplasia. While there is no ortholog of HES4 in mouse, the zebrafish ortholog *her9* provides a powerful model to study this disease. In this study we investigate the role of *her9* in zebrafish craniofacial patterning and development.

Methods: Single-cell RNA sequencing and RT-qPCR were performed to confirm *her9* is a target of *jag1b.* A *her9* mutant line from ENU mutagenesis was generated. *her9* heterozygous zebrafish were intercrossed and their offspring were skeletal prepped at 6 days post fertilization (dpf) using alizarin red and alcian blue. *her9;jag1b* double heterozygous zebrafish were intercrossed and their offspring were skeletal prepped at 6dpf. In-situ hybridization was performed in wild-type zebrafish at 48hpf using a *her9* probe. Wild-type zebrafish embryos were treated with γ-secretase inhibitor, DBZ, at three different timepoints.

Results: *her9* expression is significantly decreased in *jag1b* mutants at 48hpf but not at 28hpf (T-test). *her9* mutants alone do not produce any craniofacial patterning defects. However, they fail to make neural crest derived bone. Taking out copies of *her9* in *jag1b* mutants significantly increases the penetrance of *jag1b* mutant phenotypes (n=44, Fisher's exact). Treating embryos with DBZ fails to phenocopy *her9* mutants.

Conclusion: *her9* alone is not required for correct craniofacial patterning but it is required for neural crest derived bone development. Our data suggest that there are different gene regulatory networks required for neural crest cell derived and mesoderm derived bone development.

Funding Sources: NIH R01 DE029193

Category: Professional Research Assistant
Poster # PRA9

Title: Oral Health and HIV: Dental Students Knowledge, Attitudes, and Experiences

Caitlyn Wayment and Tamara Tobey

Background: Provider knowledge and attitudes pertaining to providing care to vulnerable populations impacts the oral care of patient living with HIV (PLWH), but oral health providers often have inadequate knowledge or stigmatized attitudes towards PLWH.
Purpose: To assess the impact of dental students participating in a lecture on medical management, oral health for persons living with HIV, and HIV prevention.
Methods*:* During the 2019-20 and 2020-21 school years, third year dental students at the University of Colorado School of Dental Medicine participated in a lecture presented by a provider at the Colorado and Mountain-West AIDS Education and Training Centers. Students completed pre- and post-intervention surveys which examined their HIV-related knowledge, attitudes and stigma towards HIV/AIDS, and educational experience.
Results: Our results of the pre-intervention survey included 113 respondents between the ages of 23-45 with an average knowledge score of 8.93 points out of 12. The post-intervention survey included 92 respondents between the ages of 24-45 reporting an average knowledge score of 9.05 points out of 12. A paired-samples t-test was conducted to compare knowledge scores in the pre- and post-educational seminar. There was a significant difference in the scores for pre-intervention (M=8.25, SD =1.42) and post-intervention (M=8.88, SD=1.46) conditions; t=2.50, p=0.014. Preliminary analyses indicate students became less concerned about contracting HIV from patients and more confident in their knowledge regarding treating PLWH.
Conclusions: The addition of an educational session on treating PLWH not only increases knowledge about treating PLWH, but also has the potential to reduce stigmatizing attitudes and beliefs surrounding PLWH.
Source of Funding: This project is supported by the Health Resources and Services Administration (HRSA) Ryan White HIV/AIDS Program, Part F: Community-Based Dental Partnership Program (CBDPP)
University of Colorado Anschutz Medical Campus Institutional Review Board: The study is exempt as approved by the University of Colorado Anschutz Medical Campus Institutional Review Board (protocol code 21-4326, exempt).